

Real-Space Determination of Atomic Structure of the Si(111)- $\sqrt{3} \times \sqrt{3}R 30^\circ$ -Au Surface by Low-Energy Alkali-Ion Scattering

K. Oura, M. Katayama, F. Shoji, and T. Hanawa

Electron Beam Laboratory, Faculty of Engineering, Osaka University, Suita, Osaka 565, Japan

(Received 12 June 1985)

The Si(111)- $\sqrt{3} \times \sqrt{3}R 30^\circ$ -Au structure has been analyzed by low-energy alkali-ion-scattering spectroscopy. It has been derived that (1) Au triplet clusters form the $\sqrt{3} \times \sqrt{3}R 30^\circ$ lattice and (2) the Si first layer of honeycomb structure lies slightly below the Au layer.

PACS numbers: 68.20.+t, 68.55.+b, 79.20.Rf

Recently, the structural characterization of metal-semiconductor (Si) interfaces has become a subject of major interest. Of particularly crucial interest are questions related to the intermixing between the metal and the Si and to the abruptness of the interface. To clarify these problems, the determination of atomic arrangements of Si substrates carrying submonolayer metallic deposits is of great importance. For the Au/Si(111) system, the formation of a series of gold-induced superstructures and the subsequent thin-film growth process have been extensively studied with use of various complementary techniques.¹ However, no conclusive structural models have been obtained as yet. In this Letter we present, for the first time, a quantitative real-space determination of the surface structure of a gold-induced superstructure, Si(111)- $\sqrt{3} \times \sqrt{3}R 30^\circ$ -Au. On the basis of impact-collision ion-scattering spectroscopy (ICISS) analysis using alkali-metal ions, we report that (1) Au triplet clusters form the $\sqrt{3} \times \sqrt{3}R 30^\circ$ lattice, and (2) the Si first layer of honeycomb structure lies slightly below the Au layer.

In the ICISS proposed by Aono *et al.*,^{2,3} the experimental scattering angle θ of low-energy noble-gas ions is taken close to 180° so as to observe ions that have made impact collisions against surface atoms with nearly zero impact parameter. Because of this specialization of the scattering condition, ICISS allows one to analyze the atomic structure of solid surfaces straightforwardly in real space. However, ICISS using noble-gas ions involves difficulties arising from the ion-neutralization effect as in conventional ISS. The difficulty can be excluded by the use of alkali-metal ions whose neutralization probability is very small, as reported by Niehus and Comsa,⁴ by Niehus,⁵ and by others.⁶ The method of alkali-metal ICISS (ALICISS) has been applied to the Au/Si system, and the results are given in this paper.

Experiments were performed in an ultrahigh vacuum system equipped with ion scattering and LEED-Auger apparatus and a metal evaporation source by which Au can be deposited at a rate of 1 monolayer/min. A Na⁺-ion source was made accord-

ing to a prescription reported by Weber and Cordes.⁷ Na⁺ primary currents of the order of 10^{-10} A or below were sufficient to obtain spectra, and are a factor of 100 to 1000 lower than noble-gas-ion (He⁺) currents. Scattered-ion intensity was measured in 7 s (which corresponds to 3.9×10^{10} ions/cm² of ion dose) per measuring point. Thus the amount of ion-induced damage and of surface contamination during measurements was practically negligible. We used a scattering angle $\theta = 140^\circ$ which we found to be large enough to yield nearly the same features as a pure-impact-collision condition of $\theta = 180^\circ$. The Si(111) sample was cleaned by repeated flashing at high temperatures. After cleaning a sharp 7×7 LEED pattern was observed, and no impurities were detected by ISS. The substrate temperature during Au deposition was 700°C , at which the sticking coefficient is nearly equal to 1, as studied by LeLay and Faurie.⁸ With an increase in the Au coverage, a series of superstructures successively appeared; the Au coverage necessary for the completion of each superstructure has been determined^{9,10} to be about 0.4, 1.0, and 1.5 monolayers (ML) for the 5×1 , $\sqrt{3} \times \sqrt{3}R 30^\circ$, and 6×6 phases, respectively, in agreement with other reports,^{1,8} where 1 ML = 7.8×10^{14} atoms/cm², the density of Si atoms in the (111) plane.

A typical energy spectrum of Na⁺ ions scattered from the Si(111)- $\sqrt{3} \times \sqrt{3}R 30^\circ$ -Au surface is shown in Fig. 1. It can be seen that the spectrum is dominated by a single peak at $E/E_0 = 0.66$ in agreement with the energetic position, 0.661, expected on the basis of the single-scattering model between Au and Na at $\theta = 140^\circ$ (a Si peak expected at $E/E_0 = 0.015$ cannot be observed presumably because of the smaller detection efficiency of the analyzer for such very low-energy ions). However, the contribution of quasi single scattering,¹¹ i.e., a small-angle scattering followed by a large-angle scattering, may be significant for the intensity of the observed peak since the energetic positions expected for such quasi single scattering are very close to the single-scattering peak (e.g., a 2° scattering followed by a 138° scattering gives $E/E_0 = 0.664$). Anyway, it is evident that the appearance of visible new peaks defi-

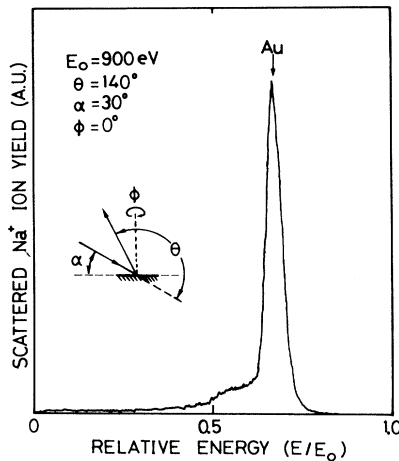


FIG. 1. Energy spectrum of Na^+ ions scattered at a large scattering angle $\theta = 140^\circ$. The arrow shows the energetic position of the single-scattering peak expected for Na-Au.

nitely separated from the single-scattering peak, as observed in conventional alkali-ion scattering^{12,13} and interpreted as due to multiple scattering involving more than two large-angle scattering processes, can be minimized in ALICISS.

The intensity of Na^+ ions scattered from Au atoms of the $\sqrt{3} \times \sqrt{3}R 30^\circ$ -Au phase in the ICISS condition is plotted in Fig. 2 as a function of the ion incidence angle measured from the surface, α , for two selected azimuthal angles, ϕ . As α increases, the Na^+ ion intensity shows a fairly steep increase at a critical angle α_c , and the features can be interpreted as follows. For $\alpha < \alpha_c$, all surface atoms are located in the shadow cones of their preceding neighbors, and hence no scattering can be observed. By an increase of α , the surface atoms step out of the shadow cone at a critical angle α_c which results in a sudden increase of the scattered ions. The most important result in Fig. 2 is that we have one α_c for $\phi = 0^\circ$, while there are two α_c 's for $\phi = 30^\circ$. The critical angle is determined by both the shape of shadow cones and the geometrical arrangement of the surface atoms.

By using the shadow cone determined from the Thomas-Fermi-Moliere potential¹⁴ for Na^+ -Au and Na^+ -Si, we have made a simple calculation in order to obtain the critical angles to be expected for various structural models. The number of Au atoms which are not concealed by shadow cones of neighboring Si and Au atoms is calculated as a function of incidence and azimuthal angles. Models involving 1 ML of Au atoms are mainly discussed here. They are (a) a triplet overlayer (TO) model proposed by LeLay and Faurie,⁸ (b) a triplet coplanar (TC) model proposed by Yabuuchi *et al.*,^{9,10} and (c) a modified triplet coplanar (MTC) model derived in this study. Other models in-

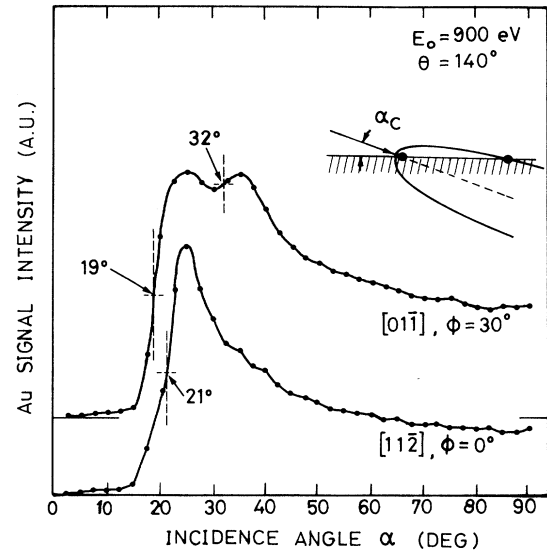


FIG. 2. Intensity of Na^+ ions scattered from Au atoms in the $\text{Si}(111)\text{-}\sqrt{3} \times \sqrt{3}R 30^\circ$ -Au surface measured in the ICISS condition as a function of the incidence angle α ; results for azimuths $\phi = 0^\circ$ and 30° are shown.

volving $\frac{1}{3}$ and $\frac{2}{3}$ ML of Au atoms are also considered for comparison. For each model, the interatomic distance, S , of Au atoms parallel to the surface and the height, H , of the Au layer relative to the Si first layer are considered as structural parameters. The atomic density of the Si first layer is also varied by a $\frac{1}{3}$ -ML step. We have assumed that one Au atom is affected by the shadow cones originating from up to the third and sixth neighbor atoms of Au and Si, respectively. Neither focusing nor thermal vibration is taken into account. The results are summarized in Table I, where critical angles α_c measured and calculated for five kinds of structural models are shown, together with the number of Au atoms responsible for each α_c . As can be seen, among these models the MTC model gives a fairly good agreement with the experiment; three α_c 's predicted for the model are observed in the experiment, but the one at 15° for $\phi = 0^\circ$ is not.

The modified triplet coplanar model that we propose for the $\sqrt{3} \times \sqrt{3}R 30^\circ$ -Au surface is shown in Fig. 3. This model is constructed by both Au triplet clusters arranged with the $\sqrt{3} \times \sqrt{3}R 30^\circ$ lattice and an underlying Si layer of honeycomb structure; the interlayer spacing between the Au and Si layers is 0.3 \AA , and the atomic density of the first layer is $\frac{2}{3}$ ML. Two α_c 's 19.1° and 30.2° , calculated for $\phi = 30^\circ$, correspond to the shadowing effect between Au atom pairs F-A (or G-B) and B-C, respectively. As α decreases, the shadowing effect of B begins first at $\phi = 30.2^\circ$ to conceal C, and then that of F (or G) at 19.1° to conceal A (or B). Thus, among the three Au atoms (e.g., atoms A, B, C

TABLE I. Critical angles α_c measured and calculated for various structural models. The number in the parentheses indicates the number of Au atoms responsible for each α_c ; the TO, TC, and MTC models involve three Au atoms in the unit cell, while there are two and one for the HC and $\frac{1}{3}$ -ML models, respectively.

Model	$\alpha_c(\phi = 0^\circ)$	$\alpha_c(\phi = 30^\circ)$
TO ^a	15°(3)	18.5°(2), 30.8°(1)
TC ^b	15°(1), 27.1°(2)	17.8°(1), 23.3°(1), 31.5°(1)
MTC ^c	15°(1), 21.2°(2)	19.1°(2), 30.2°(1)
HC ^d	15°(1), 21.5°(1)	15.5°(1), 24°(1)
$\frac{1}{3}$ ML ^e	24.9°(1)	9.5°(1)
Expt.	21 ± 0.5°	19 ± 0.5°, 32 ± 0.5°

^aTriplet overlayer model (Ref. 8), $S = 2.88 \text{ \AA}$, $H = 2.5 \text{ \AA}$. The atomic densities are Au, 1 ML, and Si, 1 ML.

^bTriplet coplanar model (Refs. 9 and 10), $S = 2.80 \text{ \AA}$, $H = 0.0 \text{ \AA}$; Au, 1 ML; Si, $\frac{2}{3}$ ML.

^cModified triplet coplanar model (this work), $S = 2.9 \text{ \AA}$, $H = 0.3 \text{ \AA}$; Au, 1 ML; Si, $\frac{2}{3}$ ML.

^dHoneycomb model, $S = 3.0 \text{ \AA}$, $H = 0.3 \text{ \AA}$; Au, $\frac{2}{3}$ ML; Si, 1 ML.

^e $\frac{1}{3}$ -ML model, $S = 3.8 \text{ \AA}$, $H = 0.3 \text{ \AA}$; Au, $\frac{1}{3}$ ML; Si, 1 ML.

of Fig. 3) involved in the $\sqrt{3} \times \sqrt{3} R 30^\circ$ unit cell of the MTC model, two Au atoms (A and B) are responsible for the critical angle at 19.1° and one Au atom (C) for the 30.2° , leading to the intensity drop at 19.1° being larger than at 30.2° , as actually observed in the experiment. The critical angle $\alpha_c = 21.2^\circ$ calculated for $\phi = 0^\circ$ is due to the shadowing effect of an underlying Si atom P (or Q) which conceals the Au atom D (or E), as illustrated in Fig. 3. Another critical angle $\alpha_c = 15^\circ$ predicted for $\phi = 0^\circ$ could not be observed in our experiment. In the calculation, the 15° α_c corresponds to the shadowing effect of Au atom F which conceals Au atom C. Though the reason for the missing angle is not clear at present, we can point out two factors which seem to reduce the shadowing effect at 15° : (1) only one Au atom is responsible for the 15° α_c , while two are responsible for the 21.2° α_c (see Table I); (2) low-energy ion scattering is sensitive to the short-range order of atomic arrangement, and hence the shadowing effect between more separated atoms is generally smaller (among the four α_c 's predicted, the 15° α_c corresponds to the most separated atom pair). In Fig. 3, the interatomic distance between B and C has been determined to be about 2.9 \AA , which is close to the most close-packed distance of bulk Au, 2.88 \AA . Though the direction of F-A (or G-B) deviates from the incident beam direction of $\phi = 30^\circ$ by about 10° , the shadowing effect of F-A (or G-B) is clearly observed because of the thick shadow cone for low-energy heavy ions [e.g., the radius of the shadow cone for a Na^+ (900 eV)-Au system is 1.6 \AA at

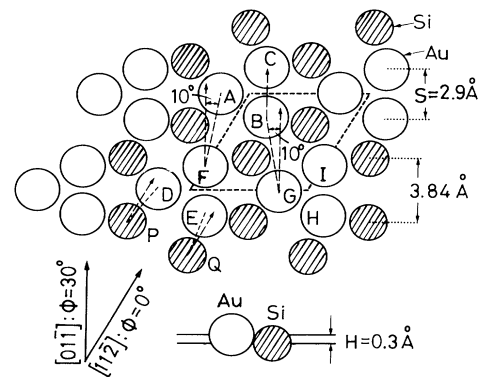


FIG. 3. New structural model for the Si(111)- $\sqrt{3} \times \sqrt{3} R 30^\circ$ -Au surface, called the modified triplet coplanar (MTC) model.

a position separated from the scatterer (Au) by 4 \AA].

The arrangement of the Au triplet cluster with the $\sqrt{3} \times \sqrt{3} R 30^\circ$ periodicity was first proposed by LeLay and Faurie⁸ on the basis of their measurement of the Au coverage (1 ML) required for the completion of this structure. The present study thus provides, for the first time, direct experimental evidence for the triplet cluster. In addition, the arrangement of the underlying Si layer has been determined in this study. Because of the rather thick shadow cone described above, the underlying Si layer can conceal the Au atom to give rise to $\alpha_c = 21^\circ$ for $\phi = 0^\circ$. For the TO model proposed by LeLay and Faurie,⁸ where the interlayer spacing between Au and Si is about 2.5 \AA , the calculated α_c for $\phi = 0^\circ$ disagrees with experiment as shown in Table I. Also, for the TC model which we have previously derived on the basis of a combined use of the LEED constant-momentum-transfer-average method and noble-gas-ion scattering, the agreement between experiment and calculation is not satisfactory. Though the TC model has been recently supported by photoelectron diffraction¹⁵ and by transmission-electron-diffraction¹⁶ experiments, it can be said that the new model described in this paper modifies our previous TC model with respect to the height of the adsorbed Au layer.

We have obtained the new model described above under the assumption of the shape of shadow cones calculated from the Thomas-Fermi-Moliere potential with $C = 0.90$.¹⁴ However, even when C is varied in the probable range of 0.80 – 1.00 , models essentially the same as shown in Fig. 3 are derived, though the height of the Au layer changes to about 0.2 and 0.4 \AA for $C = 0.80$ and 1.00 , respectively.

The authors would like to thank Mr. T. Tanabe and Mr. T. Hirose for their assistance in the experiment. One of the authors (K.O.) would like to thank Mr. H. Nakamatsu of the Scientific and Industrial Research

Institute of Osaka University for kindly supplying the sodium aluminosilicate molecular sieve used in this study. This work was partly supported by a Grant-in-Aid for Scientific Research from the Ministry of Education, Science, and Culture.

¹For a review, see G. LeLay, *Surf. Sci.* **132**, 36 (1983).

²M. Aono, C. Oshima, S. Zaima, S. Otani, and Y. Ishizawa, *Jpn. J. Appl. Phys.* **20**, L829 (1981).

³For a review, see M. Aono, *Nucl. Instrum. Methods Phys. Res. B* **2**, 374 (1984).

⁴H. Niehus and G. Comsa, *Surf. Sci.* **140**, 18 (1984).

⁵H. Niehus, *Surf. Sci.* **145**, 407 (1984).

⁶M. Aono, R. Souda, C. Oshima, and Y. Ishizawa, in *Proceedings of the First International Conference on the Structure of Surfaces*, Berkeley, 1984 (to be published).

⁷R. E. Weber and L. F. Cordes, *Rev. Sci. Instrum.* **37**, 112

(1966).

⁸G. LeLay and J. P. Faurie, *Surf. Sci.* **69**, 295 (1977).

⁹Y. Yabuuchi, Ph.D. thesis, Osaka University, 1984 (unpublished).

¹⁰Y. Yabuuchi, F. Shoji, K. Oura, and T. Hanawa, *Surf. Sci.* **131**, L412 (1983), and to be published.

¹¹See, for example, B. M. DeKoven, S. H. Overbury, and P. C. Stair, *Phys. Rev. Lett.* **53**, 481 (1984).

¹²T. Von dem Hagen and E. Bauer, *Phys. Rev. Lett.* **47**, 579 (1981).

¹³H. Hemme and W. Heiland, *Nucl. Instrum. Methods Phys. Res. B* **9**, 41 (1985).

¹⁴The Thomas-Fermi screening radius a_{TF} is slightly modified, and the effective screening radius $a_{eff} = a_{TF}C$ is used in this study, where C is a scaling factor. The value of $C = 0.90$ is adopted here, and the effect of C on the analysis is also examined (see text).

¹⁵K. Higashiyama, S. Kono, and T. Sagawa, paper presented at the Fortieth Annual Meeting of the Physical Society of Japan, Kyoto, April 1985 (unpublished).

¹⁶M. Takahashi, K. Takayanagi, Y. Tanishiro, S. Takahashi, and K. Yagi, in Ref. 15.